Chapter 5

Statistics of the Nonlinear Distortion

In this chapter, some interesting aspects on the probability distribution of the OFDM signal and its relations with nonlinear distortion and clipping effects are reviewed. The possibility of a CDF based estimation of the AM/AM pre-distortion characteristic is also presented discussing the influence of the time delay in AM/PM compensation.

5.1   Simplified model including time delay

Along the previous chapters we provided a detailed signal and system model which is needed to justify the higher level approximations used in our linearization problem and to achieve a deeper understanding of the transmission structure under the effect of a nonlinearity. Now, the present discussion is focused as an intermediate analytical step between the theoretical signal models and the formulation of the linearization algorithms. For this purpose, we review the basic model initially presented in section 3.1.1. In equation (3.2) we defined the continuous-time OFDM symbol as

$$b_x(t) = \frac{1}{\sqrt{N}} \sum_{k=0}^{N-1} d_x(k,i) e^{j2\pi f_k t}, \ \ \text{for } t \in \mathcal{I}_i$$

whit f_k the k-th carrier frequency and $d_x(k,i)$ the M-QAM symbol modulating the k-th carrier during the i-th OFDM symbol interval. The transmission of this base-band signal is considered in the simplified block diagram of a generic OFDM system shown in figure 5.1 where the nonlinear distortion introduced by the HPA block in RF can be modeled in base-band according to the memoryless I/O relations given in chapter 2. Nevertheless, the up and down-conversion chains therein included, encompass analog pass-band filters that introduce an important group delay at the signal which, in addition to the inherent HPA's memory, contributes to a total time misalignment between $b_x(t)$ and $b_y(t)$. Therefore, an effective time delay between the input $b_x(t)$ and output $b_y(t)$ base-band signals must be
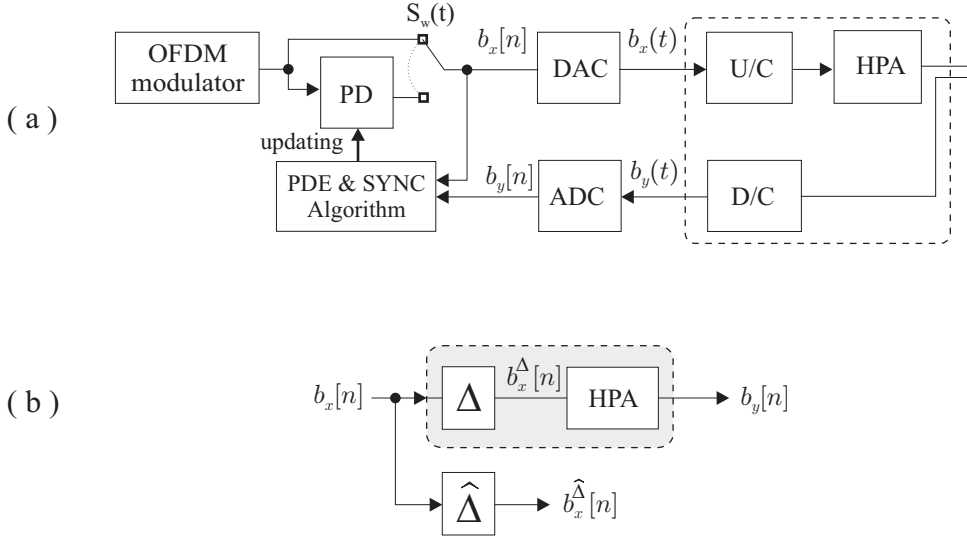
Figure 5.1: (a) Simplified block diagram of the pass-band OFDM system model including adaptive PD estimation (b) Base-band model of the HPA including memory effect.

considered and, whenever necessary, compensated to estimate the PD characteristic. Such time delay is also registered between the discrete versions of the base-band signals, $b_x[n]$ and $b_y[n]$, available at the input and the output of DAC and ADC, respectively. This effect is implicit to those elements within the dash-lined block in figure 5.1(a) where the transmitter and receiver block diagram of the pass-band OFDM system is shown. Then, in figure 5.1(b), the time delay is explicitly represented as the concentrated parameter

$$\Delta = T_s \Delta_{int} + \Delta_{frac},$$

associated to the memoryless HPA model. The total time delay may be composed of an integer and a fractional part in terms of the sampling time T_s. While the fractional misalignment can be compensated by inserting adaptive filters or interpolators, the integer or coarse time delay Δ_{int} can be effectively compensated through a Time Delay Estimation (TDE) procedure like [54],[39] or [38] for TDE and synchronization before the pre-distortion process.

If the bandwidth of the analog up/down-conversion filters is deemed reasonably superior to the bandwidth of the OFDM signal in incorporating the significant excess side-band components due to spectral re-growth from the PD and HPA nonlinear operations, the final nonlinear distortion base-band model in discrete time can be approximated with the following relationships:

$$
\begin{aligned}
b_y(n) &= b_x(n - \Delta) \cdot \mathrm{HPA}[u_x(n - \Delta)] \\
&= A[u_x(n - \Delta)]\, e^{j\left[\alpha_x(n-\Delta) + \Phi[u_x(n-\Delta)]\right]} \\
&= u_x(n - \Delta) G_{AM}[u_x(n - \Delta)]\, e^{j\left[\alpha_x(n-\Delta) + \Phi[u_x(n-\Delta)]\right]} \\
&= u_y(n)\, e^{j\,\alpha_y(n)}
\end{aligned}
\tag{5.1}
$$

where $A[\cdot]$ and $\Phi[\cdot]$ represent the AM/AM and AM/PM distortions respectively. Hence, in order to apply digital pre-distortion to obtain linearization, it may be necessary to estimate Δ to ultimately find a discrete inverse multiplicative function $\text{HPA}^{-1}[\cdot]$ such that, $b_x(n - \Delta) = b_y(n) \cdot \text{HPA}^{-1}[u_y(n)]$.

5.2 Statistics of distortion and clipping effect

From section 2.2.1, equations (2.30) and (2.31), we have the expressions for the direct and inverse AM/AM characteristic of the Saleh model respectively given by

$$A[u_x] = \frac{A_s^2 \alpha_a u_x}{A_s^2 + u_x^2}$$

and

$$A^{-1}[u] = \frac{\alpha_a A_s^2}{2u}\left[1 - \sqrt{1 - \left(\frac{2u}{\alpha_a A_s}\right)^2}\right]$$

where it is important to note again that this theoretical inversion remains valid only within the interval $[\,0 \leq u \leq \alpha_a A_s/2\,]$ that defines the under-saturation input-output dynamic range of the HPA. Recall that this range was previously normalized to $[0, 1]$ when the HPA model for simulations was presented in chapter 2.2.

According to the typical hypothesis of statistical independence, the complex symbols $d_x(k)$ in (3.2) are considered mutually independent and identically distributed (i.i.d.) symbols for any time interval. A complementary assumption is that the signal power is uniformly distributed over the N OFDM sub-carriers using the same QAM constellation for each one of them. Thence, for large values of N (> 30) and by means of the Central Limit Theorem, the CDF of $b_x(t)$ can be well approximated by that of a two-dimensional complex Gaussian random process, with zero-mean and variance $2\sigma^2$. Consequently, the envelope of this signal $u_x(t) = |b_x(t)|$ can be considered as Rayleigh distributed and, since the in-phase and in-quadrature components are uncorrelated, the phase information $\text{Arg}\{b_x(t)\} = \alpha_x(t)$ is uniformly distributed in the interval $[-\pi, \pi]$. The theoretic PDF-CDF pair for the Rayleigh distribution of the input modulus $u_x(t)$ is given by

$$p_{Rayl}(u) = \frac{u}{\sigma^2}\exp\{-\frac{u^2}{2\sigma^2}\} \tag{5.2}$$

$$F_{Rayl}(u) = 1 - \exp\{-\frac{u^2}{2\sigma^2}\} \tag{5.3}$$

with mean $\mu_{Rayl} = \sigma\sqrt{\frac{\pi}{2}}$ and variance $\sigma_{Rayl}^2 = \frac{4-\pi}{2}\sigma^2$. The corresponding theoretical inverse for the distribution function in (5.3) can be easily calculated as

$$F_{Rayl}^{-1}(u) = \sigma\sqrt{2\ln\left(\frac{1}{1-u}\right)}. \tag{5.4}$$
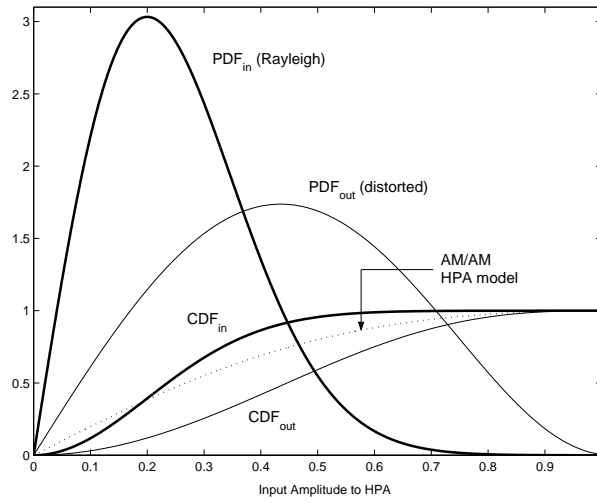
Figure 5.2: Input-to-output alteration of a Rayleigh distribution ($\sigma = 0.2$) due to the AM/AM non-linear distortion introduced by the normalized Saleh model of HPA.

Then, according to the analytical correspondence defined in (2.31), the PDF of the distorted data at the output of the HPA can be expressed as follows:

$$p_{dist}(u) = \frac{p_{Rayl}\left(A^{-1}[u]\right)}{\dot{A}\left[A^{-1}[u]\right]} \tag{5.5}$$

where $\dot{A}[\cdot]$ stands for the derivative of the AM/AM transfer characteristic (2.26) with respect to u_x. This function is given by

$$\dot{A}[u] = \frac{\partial A[u]}{\partial u} = \alpha_a A_s^2 \left[\frac{A_s^2 - u}{(A_s^2 + u^2)^2}\right]. \tag{5.6}$$

Since the transfer AM/AM curve tends to concentrate the output probability density in zones where the gradient of $A[u]$ tends to lower values, $\dot{A}[\cdot]$ operates as a scaling factor to redistribute the PDF preserving the same total probability, so that $F_{Rayl}(\infty) = F_{dist}(\infty) = 1$. Then, the output CDF can be obtained as the integral of $p_{dist}(u)$ or by direct replacement of (2.31) into (5.3), i.e. $F_{dist}(u) = F_{Rayl}(A^{-1}[u])$, where no scaling will be necessary. In figure (5.2) these analytical relationships are graphically shown for this particular case, where Rayleigh distributed samples of the input signal amplitude $u_x(t)$ are highly AM/AM distorted using (2.26). Since, from (5.3) we have that $F_{Rayl}(5\sigma) = 0.9999963$, letting $\sigma = 0.2$ almost every signal sample at the input distribution will be located within the normalized dynamic range $[0, 1]$. Therefore a good condition for digital data treatment when dealing with Rayleigh distributed OFDM sampled data would be to require that the input signal power with respect to the saturation input amplitude satisfy $A_s \leq 5\sigma$. For practical applications, regarding the limited (and non-linear) dynamic response of A/D and D/A converters, it is a common practice to use $3\sigma \leq A_s \leq 6\sigma$ for OFDM signals with M-QAM modulated subcarriers.
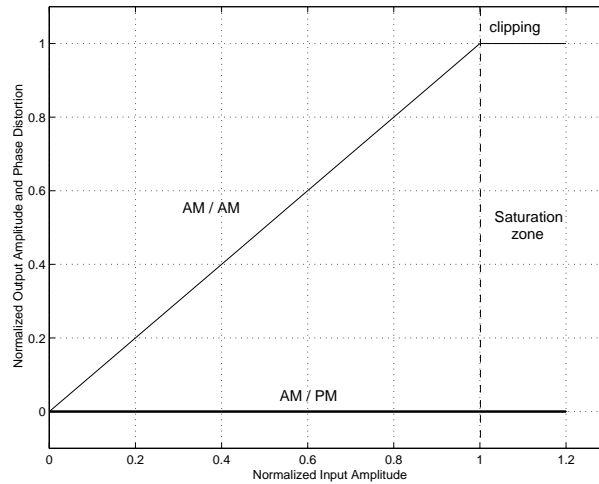
Figure 5.3: Ideally pre-distorted HPA characteristics.

5.2.1 Clipping characterization

From the discussion presented in section 2.2.2 we have established that, even if the ideal pre-distorter is applied, whenever the signal envelope distribution has a non-null probability for inputs exceeding the saturation point, it will not be possible to avoid the non-recoverable distortions due to the amplitude limiting behaviour of the linearized HPA [55]. Indeed, the only manner to preclude clipping degradation is to restrict almost 100% of the signal probability density to be within the valid input range $[0, A_{sat}]$. In practice, when dealing with a distribution with a large peak-to-mean ratio, as is the case of the Rayleigh distribution, this restriction means a severe reduction of the input power and consequently an important efficiency loss for the HPA operation. Therefore, it is important to quantify the relations between the statistical distribution of the OFDM signal and the expected power losses and noise due to the clipping effect in order to properly asses the final results of any linearization scheme. The theoretical relations presented in this section are intended to provide insight to some of the expectable system degradations in the upcoming algorithm simulations.

Assuming the ideal pre-distorter has been achieved, the linearized combination PD+HPA will behave as the ideal unitary gain amplitude limiter device (AM/AM clipper) shown in figure 5.3. This ideal AM/AM limiter characteristic is defined by

$$C(u) = \left\{ \begin{array}{ll} u & ; \quad 0 \leq u < A_{sat} \\ A_{sat} & ; \quad u \geq A_{sat}. \end{array} \right. \tag{5.7}$$

where A_{sat} is the maximum output amplitude allowed. Along with this, the AM/PM characteristic of the linearized combination will be considered ideal, that is, it does not introduce any phase modifications to the input base-band signal $b_{in} = ue^{j\phi}$, for any value of the modulus $u = |b_{in}|$.
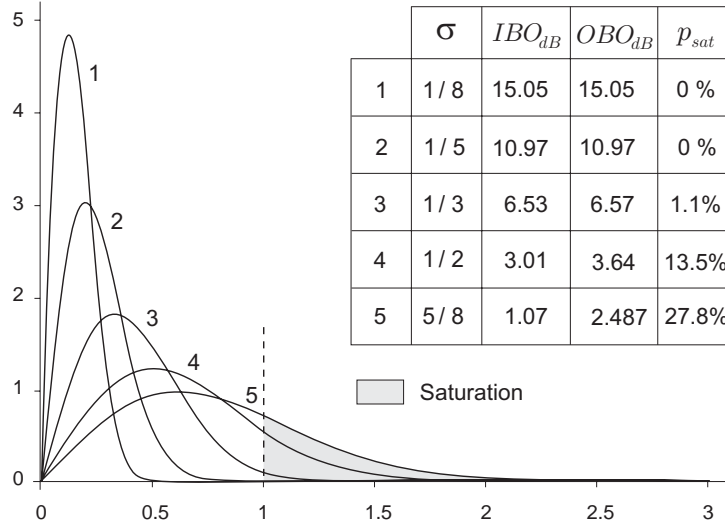
σ	IBO_{dB}	OBO_{dB}	p_{sat}
1	1 / 8	15.05	15.05	0 %
2	1 / 5	10.97	10.97	0 %
3	1 / 3	6.53	6.57	1.1%
4	1 / 2	3.01	3.64	13.5%
5	5 / 8	1.07	2.487	27.8%

Figure 5.4: Rayleigh distributions with different mean power and their clipping probabilities.

The input and output signals of an ideal limiter are typically considered to define the input and output back-off for an HPA operation as follows:

$$IBO_{dB} = 10\log_{10}\left(\frac{P_{max}}{\overline{P}_{in}}\right) \tag{5.8}$$

$$OBO_{dB} = 10\log_{10}\left(\frac{P_{max}}{\overline{P}_{out}}\right) \tag{5.9}$$

where P_{max} is the maximum output power that, in this case, has been normalized by the input saturation power so that $P_{max} = A_{sat}^2 = 1$. The mean input power defined for the Rayleigh distribution in (5.2) is $\overline{P}_{in} = 2\sigma^2$. Thence, the IBO can be expressed alternatively[1] as

$$IBO = \frac{A_{sat}^2}{2\sigma^2} \tag{5.10}$$

$$IBO_{dB} = 10\log_{10}\left(\frac{A_{sat}^2}{2\sigma^2}\right). \tag{5.11}$$

Using the definition of the Rayleigh CDF given in (5.3), the probability of saturation of the OFDM base-band signal envelope, expressed as the random variable u, can be calculated as

$$p_{sat} = p(u \geq A_{sat}) = 1 - F_{Rayl}(A_{sat}) = e^{-\frac{A_{sat}^2}{2\sigma^2}} = e^{-IBO}. \tag{5.12}$$

---

[1]The related parameters IBO (ratio) and IBO_{dB} (ratio in dB) will appear conveniently included in some equations. Note that their numerical values are not equivalent for calculations.

In figure 5.4, given the normalized saturation level $A_{sat} = 1$, we show the Rayleigh PDFs for different levels of IBO, indicating the probability of saturation ($p_{sat} \cdot 100\%$) for each case. Assuming that there are no power losses due to temperature dissipation, signal insertion and so on, the total mean input power $\overline{P}_{in}$ can be divided at the output of the limiter (PD+HPA) into two portions which are expressed as

$$\overline{P}_{in} = \overline{P}_{lin} + \overline{P}_{clip}. \tag{5.13}$$

Here $\overline{P}_{lin}$ corresponds to the power of the portion of signal which is linearly transferred (non-clipped) to the output, while $\overline{P}_{clip}$ expresses the mean power of that portion of the input signal which will undergo clipping after passing through the linear limiter. This value can be calculated using (5.2) as

$$\begin{aligned}
\overline{P}_{clip} &= \int_{A_{sat}}^{\infty} u^2 p_{Rayl}(u) du \\
&= \int_{A_{sat}}^{\infty} \frac{u^3}{\sigma^2} e^{-\frac{u^2}{2\sigma^2}} \\
&= (A_{sat}^2 + 2\sigma^2) e^{-\frac{A_{sat}^2}{2\sigma^2}}.
\end{aligned} \tag{5.14}$$

Now, under a worst case criterion, the clipping effect may introduce a critical distortion level making the transmitted information associated to the clipped portion of the signal unrecoverable. Thus we can define a signal-to-clipped-noise ratio as a measure of the extreme clipping degradation in terms of the IBO. This parameter is calculated as

$$\begin{aligned}
SNR_{clip} &= 10 \log_{10} \left(\frac{\overline{P}_{in}}{\overline{P}_{clip}} \right) \\
&= -10 \log_{10} \left(\frac{(A_{sat}^2 + 2\sigma^2) e^{-\frac{A_{sat}^2}{2\sigma^2}}}{2\sigma^2} \right) \\
&= -10 \log_{10} \left(e^{-\frac{A_{sat}^2}{2\sigma^2}} \left(1 + \frac{A_{sat}^2}{2\sigma^2} \right) \right) \\
&= -10 \log_{10} \left(e^{-IBO} (1 + IBO) \right).
\end{aligned} \tag{5.15}$$

In figure 5.5 we show a depiction of the relation expressed in (5.15) but showing the dependence of SNR_{clip} with respect to the IBO_{dB}. This can be used as a reference if, for example, we require the clipped power to be 60dB below the mean input power, then we have to set an $IBO > 12$dB (actually ≥ 12.246dB).

The separation of power terms in equation (5.13) establishes that after clipping an efficiency degradation is introduced in terms of the output power. Such degradation can be observed through the difference between IBO and OBO. For this purpose, let us first consider that the power of the non-clipped portion of the signal at the output of the limiter is given by
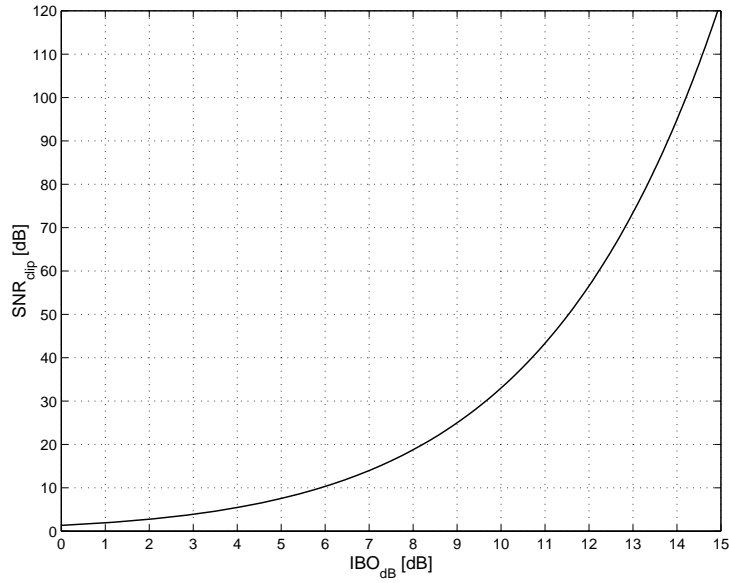
Figure 5.5: Relation between the Signal-to-clipped-noise ratio SNR_{clip} and IBO_{dB}.

$$\overline{P}_{lin} = \overline{P}_{in}F(A_{sat}) = 2\sigma^2(1 - e^{-\frac{A_{sat}^2}{2\sigma^2}}) = \overline{P}_{in}(1 - e^{-IBO}). \tag{5.16}$$

Then, we can formulate the following relations that define the OBO:

$$
\begin{aligned}
OBO_{dB} &= 10\log_{10}\left(\frac{P_{max}}{\overline{P}_{lin}}\right) \\
&= 10\log_{10}(P_{max}) - 10\log_{10}(P_{out}) \\
&= 10\log_{10}(P_{max}) - 10\log_{10}\left(\overline{P}_{in}(1 - e^{-IBO})\right) \\
&= 10\log_{10}\left(\frac{P_{max}}{\overline{P}_{in}}\right) - 10\log_{10}\left(1 - e^{-IBO}\right) \\
&= IBO_{dB} - 10\log_{10}\left(1 - e^{-IBO}\right) \tag{5.17}
\end{aligned}
$$

Thus, with the relations above, we can evaluate the OBO as a parameter dependent from the IBO. This dependence is shown in figure 5.6 where we can observe that for small values of IBO, which implies high probability of saturation, the OBO curve tends to $OBO \approx 0$ while, for IBO values greater than 10dB, which implies a very low saturation probability, the IBO and OBO values tend to be equal and hence the system degradation due to clipping can be neglected in the performance assessment of the linearizer.

Finally, another relevant measure must be formulated analytically given its utility in linearization assessment and also to avoid confusion in interpreting the power parameters included up to this point. In an ideal linear transference with no AM/PM distortion and
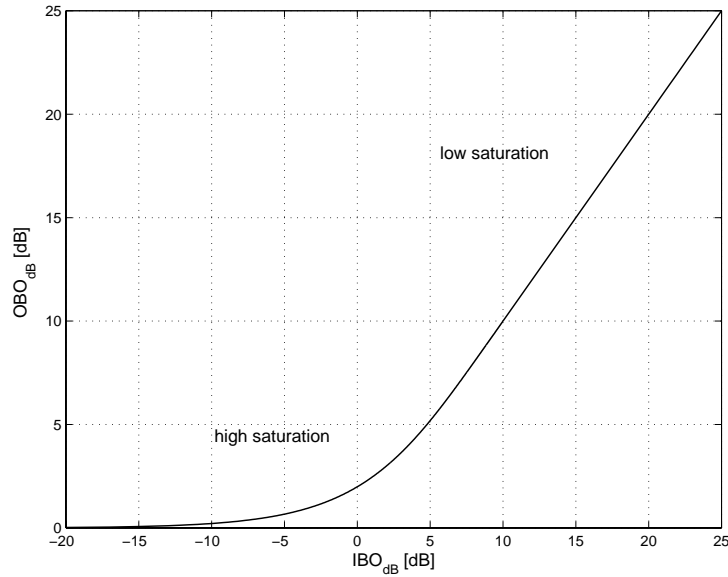
Figure 5.6: Output back-off in dependence of Input back-off in dB.

where the AM/AM clipping of the input signal envelope to a given A_{sat}, as expressed in (5.7), is the only source of input-to-output error, the resulting clipping error signal

$$e_c = (u - C(u))e^{j\phi} \tag{5.18}$$

with ϕ the undistorted input phase, is a measure of the maximum correction limit that can be achieved by means of a pre-distortion linearizer which cannot counteract clipping distortions over saturation. Therefore, after some calculations shown in appendix 5.A, the mean power of the cliiping error signal in (5.18) can be expressed as

$$\boxed{\overline{P}_{Eclip} = 2\sigma^2 e^{-\frac{A_{sat}^2}{2\sigma^2}} - \sigma\sqrt{2\pi}A_{sat}\,\text{erfc}\left(\frac{A_{sat}}{\sigma\sqrt{2}}\right)} \tag{5.19}$$

for the particular case when the linear clipper input is driven with a signal with Rayleigh distributed envelope of variance $2\sigma^2$. This measure, for a given A_{sat}, is a function of the input power and, therefore, can be also expressed as a function of IBO

$$\overline{P}_{Eclip} = \frac{A_{sat}^2}{IBO}e^{-IBO} - \sqrt{\frac{\pi}{IBO}}A_{sat}^2\,\text{erfc}\left(\sqrt{IBO}\right). \tag{5.20}$$

Then, with the mean input power defined for the Rayleigh distribution as $\overline{P}_{in} = 2\sigma^2$ and using (5.19) we can finally express the ratio

$$\boxed{(\overline{P}_{Eclip}/\overline{P}_{in})[dB] = 10\log\left(\frac{\overline{P}_{Eclip}}{\overline{P}_{in}}\right)} \tag{5.21}$$
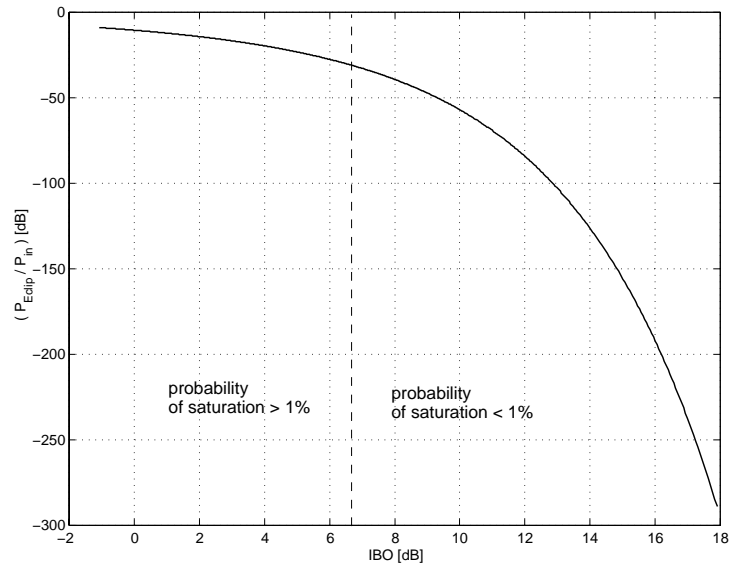
Figure 5.7: Theoretical lower bound for the power of the I/O clipping error signal normalized to the input power as a function of IBO. The input signal has Rayleigh distributed envelope and is applied to the ideal limiter specified in equation (5.7).

which is the lower bound expressing the minimum level of error signal power normalized to the input power of an input with Rayleigh distributed amplitude, in presence of a linear clipper with the maximum output power defined by A_{sat}^2. In figure 5.7 we depict this important relation that will be used later for reference to evaluate the PD simulation results.

5.3 CDF based Pre-distortion

This section shows the relationships that govern the estimation of the direct and inverse characteristic of the HPA in terms of the cumulative density functions (CDF) of the signals $b_x[n]$ and $b_y[n]$. The application of Ordered Statistics based estimation is well established for AM/AM identification and it is shown that a joint estimation of the Pre-Distortion characteristic and Time Delay Δ is required when considering the AM/PM effect.

From equations (5.1) we have the AM/AM and AM/PM correspondences given by

$$u_y(n) = A(u_x[n - \Delta]) \tag{5.22}$$
$$\alpha_y(n) = \alpha_x[n - \Delta] + \Phi[u_x[n - \Delta]]. \tag{5.23}$$

The aim here is to determine the relationship between these correspondences and the changes in the statistical distribution of the signal from the input to the output of the nonlinearity.

5.3.1 Identification of AM/AM Pre-Distortion

From equation (5.22), we can define the probability density function of $u_x(n - \Delta)$ and $u_y(n)$ as $p_{in}(u_x)$ and $p_{out}(u_y)$, respectively. Note that in terms of the PDF, the parameter Δ is irrelevant. Then, we have that the input and distorted densities fulfil

$$\int_0^{u_x} p_{in}(u)du = \int_0^{A[u_x]} p_{out}(u)du \tag{5.24}$$
$$\int_0^{u_y} p_{out}(u)du = \int_0^{G^{-1}[u_y]} p_{in}(u)du. \tag{5.25}$$

Then, assuming perfect reciprocity of the normalized non-linear direct and inverse AM/AM transfer characteristics within the interval $[0, 1]$, we have that $A^{-1}[u_y] = u_x$. By applying the integral definition of CDFs and denoting them as F, with $F_{in}(0) = F_{out}(0) = 0$ (because $u \geq 0$ by definition), we can express (5.24) and (5.25) with the corresponding distribution functions

$$F_{in}(u_x) = F_{out}(G[u_x]) \tag{5.26}$$
$$F_{out}(u_y) = F_{in}(G^{-1}[u_y]). \tag{5.27}$$

Having the input and output modulus u_x and u_y normalized to the same dynamic range $[0, 1]$, it is possible to obtain from (5.26) and (5.27), without loss of generality, the following set of common variable expressions:

$$A[u] = F_{out}^{-1}(F_{in}(u)) \tag{5.28}$$
$$A^{-1}[u] = F_{in}^{-1}(F_{out}(u)) \tag{5.29}$$

where the direct and inverse AM/AM non-linear characteristics $A[u]$ and $A^{-1}[u]$ are finally expressed in terms of the input and output CDFs of the modulus. Hence, any procedure preserving the CDF information, such as the use of Order Statistics of the modulus, is capable of estimating the AM/AM PD characteristic. Note that, for this purpose, knowledge of Δ is clearly superfluous.

5.3.2   Identification of AM/PM Pre-Distortion

Along the same lines, the PDF of the output phase $\alpha_y(n)$ can be obtained from equation (5.23) as the following circular convolution operation:

$$p_{\alpha_y}(\alpha_y) = \int_{-\pi}^{+\pi} p_{\alpha_x}(\theta) p_\Phi(\alpha_y - \theta) d\theta \tag{5.30}$$

with $p_{\alpha_x}(\theta)$ and $p_\Phi(\phi)$ the PDFs of the statistically independent variables $\alpha_x[n]$ and $\Phi[u_x[n]]$ respectively. But, as the PDF of $\alpha_x[n]$ is uniform, this results in

$$p_{\alpha_y}(\alpha_y) = \int_{-\pi}^{+\pi} \frac{1}{2\pi} p_\Phi(\alpha_y - \theta) d\theta = \frac{1}{2\pi} \tag{5.31}$$

being also uniform for any $\Phi[\cdot]$. Hence, identification of AM/PM pre-distortion is not possible from the phase alone. AM/PM pre-distortion can only be determined if the phase term $\alpha_x(n-\Delta)$ in (5.23) can be substracted from the phase $\alpha_y(n)$ to preclude the circular averaging in equation (5.31). This correspond to the straightforward identification

$$\alpha_y(n) - \alpha_x(n - \Delta) = \Phi[u_x(n - \Delta)] \tag{5.32}$$

which is only possible if the time delay Δ is known. Hence, synchronization between $b_x(n)$ and $b_y(n)$ is necessary in the presence of AM/PM distortion.

5.3.3   CDF Estimation using Order Statistics

In view of the last results, the application of Ordered Statistics to CDF estimation and AM/AM pre-distortion is introduced in this sub-section.

When the (stationary) input probability distribution is known a priori, as in (5.3), a simple fixed pre-distortion design can be implemented by replacing the known $F_{in}^{-1}(\cdot)$ in (5.29). The estimation task is thus reduced to finding the variance σ^2 of the input signal and the output CDF. Nevertheless, in a general context, no a priori knowledge on the input and output distributions is assumed to guarantee full adaptability. Thence, for the estimation of AM/AM pre-distortion using the general property expressed in equation

(5.29), a frame-oriented processing algorithm can be described as follows in general terms for any variable x:

1. A pair of input and output discrete signal vectors, $\mathbf{x}_{in}[n]$ and $\mathbf{x}_{out}[n]$ respectively, are acquired at each iteration $m = \{1, 2, \cdots\}$, as N-sample long data-blocks, defined as

$$\mathbf{x}_{in[N]}(m) = \quad [x_{in(1+(m-1)N)}, \cdots, x_{in(mN)}]^T \tag{5.33}$$

$$\mathbf{x}_{out[N]}(m) = \quad [x_{out(1+(m-1)N)}, \cdots, x_{out(mN)}]^T. \tag{5.34}$$

2. The distributions $F_{in}^{-1}(\cdot)$ and $F_{out}(\cdot)$ are estimated separately during the same m-th interval of discrete time $\{1 + (m-1)N \leq n \leq mN\}$.

3. Finally, the estimated distributions can be used according to (5.29) to interpolate $A^{-1}[\cdot]$ thus pre-distorting the input frame $\mathbf{x}_{in}(m+1)$ at the next iteration.

In scenarios where a non-stationary input distribution is considered, the estimation of the input and output CDFs will be used to adapt the PD characteristic at each iteration. However, even if the input distribution is stationary, an iterative process is suggested to update and improve the estimation of $F_{in}^{-1}(\cdot)$ and $F_{out}(\cdot)$ thus accounting for inputs with low probability values wich constitute an important source of errors as will be seen in chapter 6. The length N of the information blocks required to achieve a good linearization will depend on how the estimation of the input and output CDFs is performed.

Order Statistics (OS) filtering [56] is an efficient means to obtain an estimation of the inverse distribution function. Basically, it can be demonstrated that the linear combination of a sorted data set provides, through suitable correspondences and normalizations, a raw estimation of the percentiles that define its direct and inverse cumulative density functions (CDF). Since in our formulation we have normalized the input-output dynamic range so that $0 \leq |x_{in}| \leq 1$ and $0 \leq |x_{out}| \leq 1$, the base of OS estimation of the distribution functions can be defined as a generalized property. For a N-length vector $\mathbf{x}_{[N]} = [x_{(1)} \cdots x_{(N)}]^T$, sampled from any original distribution with PDF $p(x)$, we obtain a sorted version $\mathbf{x}'_{[N]}$ defined as

$$\mathbf{x}'_{[N]} = [x'_{(1)} \cdots x'_{(N)}]^T \quad ; \quad x'_{(n)} \leq x'_{(n+1)}. \tag{5.35}$$

Then it can be proved that $\forall\, n = \{1, \cdots, N\}$,

$$\boxed{x'_{(n)} \;\longrightarrow\; F^{-1}\left(\frac{n}{N}\right) \Leftrightarrow N \to \infty} \tag{5.36}$$
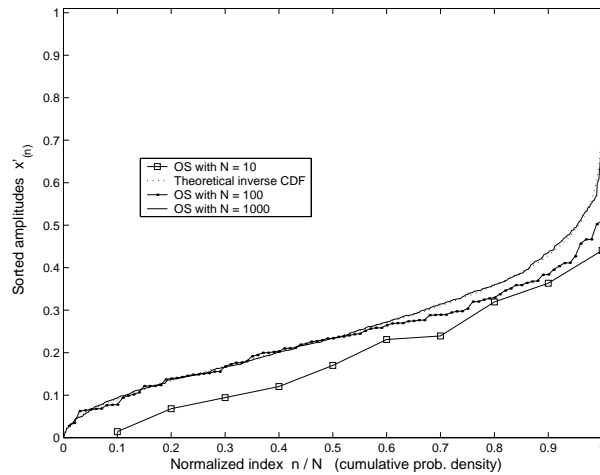
Figure 5.8: Order Statistics based CDF estimations using N = 10,100 and 1000 samples of a Rayleigh distributed RV.

where the n-th term of the sorted data vector, tends to the theoretical inverse CDF value associated to the corresponding index n normalized to the vector length. In other words, the sorted set of signal samples $\mathbf{x}'_{[N]}$ can be considered as an estimate of the percentile curve of the underlying inverse distribution $F^{-1}(x)$, provided that the number of estimated percentile points is equal to the number of elements in the sorted vector. Hence, under the assumption that the data is acquired as a sequence of i.i.d. samples of a random variable x, the one-to-one mapping $(n/N) \mapsto x'_{(n)}$ converges towards $F^{-1}(x)$ for large N. The reciprocal mapping $x'_{(n)} \mapsto (n/N)$ converges in turn towards $F(x)$. In spite of the apparent simplicity of this relationship some aspects require a review for their correct application in estimation. To provide an idea of the coarse correspondence defined in (5.36), we illustrate in figure 5.8 the resulting approach for three different sample data vector lengths. In the figure, the direct and inverse CDFs can be easily observed by simply swapping the axes. The values therein used were sampled from a normalized Rayleigh distributed signal with $\sigma = 0.2$.

From the example in figure 5.8 we can observe that the approximation of the distribution function (amplitude vs. cumulative probability) corresponds to a single-valued assignment. However, the approximation of the inverse distribution function (cumulative probability v/s amplitude) which is the displayed axis position in the figure, can be a non-unique assignment. Thus, for a finite N-sample sorted set, when $x'_{(n)} = x'_{(n+1)}$ we have that $F(x'_{(n)}) = F(x'_{(n+1)})$ and therefore, $P \leq N$ coordinated points can be defined for the approximation of direct and inverse CDFs.

In general, the PDF of an ordered statistic set from N independent identically distributed samples of a random variable is defined as ([57] chap.8)
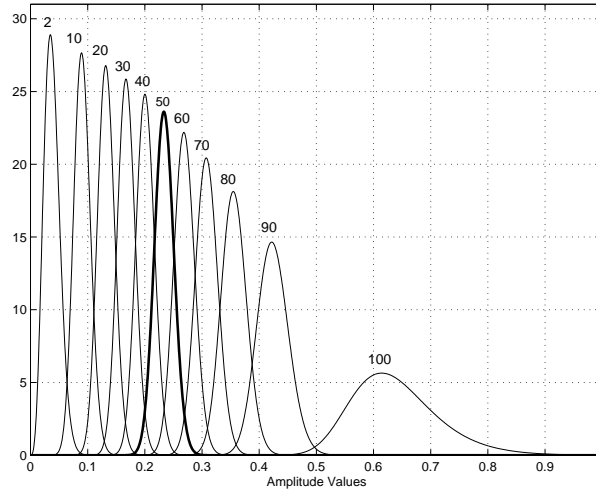
Figure 5.9: PDFs of OS percentile estimation for $r = 2, 10, 20, \cdots, 100$ using a vector of length N=101 sampled from a Rayleigh distribution $p_{Rayl}(x)$.

$$p_r(x) = \frac{N!}{(r-1)!(N-r)!} F_x^{r-1}(x) \left[1 - F_x(x)\right]^{N-r} p_x(x) \tag{5.37}$$

where $p_x(x)$ and $F_x(x)$ are the parental PDF and CDF according to which the samples in the N-sample long vector $\mathbf{x}_{[N]}$ are theoretically distributed. Since the rank index r is an integer value from 1 to N, we can obtain the PDF for the estimation of N different percentiles given by $p = 100(r/N)$. An illustrative example is shown in figure (5.9) which uses a sorted set of N=101 samples of a Rayleigh distributed signal with $\sigma = 0.2$. Since N=101 the rank index r in (5.37) indicates directly the estimated percentile p such that the 50% cumulative probability correspond to $r = 51$. According to the Rayleigh PDF and CDF distributions, shown in figure (5.2), it can be observed that the estimation of those percentiles further away from the zone in which the probability density is highly concentrated are more strongly biased (this affects the pre-distortion of the low probability range of the input data). In turn, the highlighted PDF therein shown for the estimation of the percentile 50 behaves symmetrically and features low variance around its corresponding theoretical value $F_{Rayl}^{-1}(0.5) = \sigma\sqrt{\ln 4} = 0.2355$. A more detailed study of the raw OS percentile estimation performance can be found in [58]. In the scope of our applications, a sufficient reference on the accuracy of the OS based estimation of the CDF and its inverse can be established by observing the MSE

$$\mathcal{E}(N) = \frac{1}{N} \sum_{n=1}^{N} \left| F^{-1}\left(\frac{n}{N}\right) - x'_{(n)} \right|^2 \tag{5.38}$$

resulting from the OS based estimation of the inverse distribution function in (5.4) with respect to the sorted vector of length N applied for the approximation. The results for the evaluation of this average error are shown in the upper part of figure 5.10 where we can observe, for instance, that the length $N = 1000$, previously used in figure 5.8, provides a
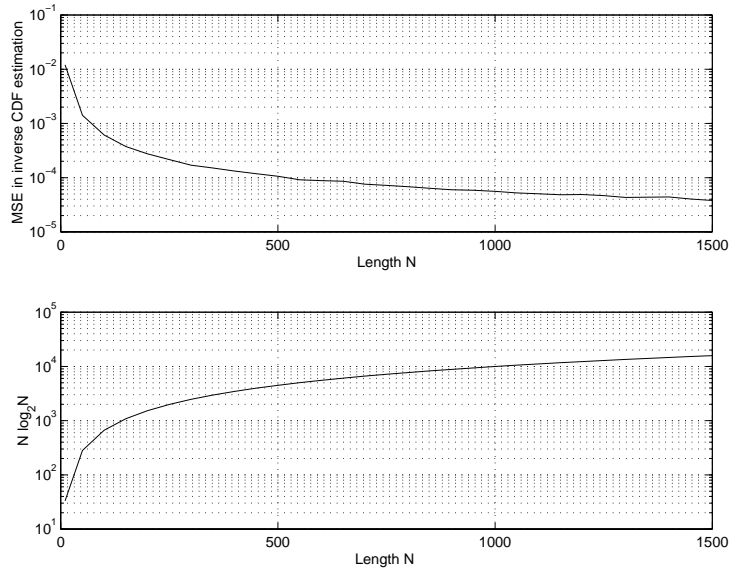
Figure 5.10: Upper: Mean Square Error for the estimation of the inverse CDF Rayleigh as a function of the length N of the Order Statistics vector. Lower: The average complexity $\mathcal{O}(N\log_2 N)$ of a Quick Sort type algorithm for the tested range of sorting lengths.

good fitting level ($\mathcal{E} \approx 10^{-4}$) with respect to the theoretical curve. Along with this, and since the feasibility of any real time application will depend also on the computational complexity of each implemented solution, in the lower part of figure 5.10 we included a depiction of the average complexity order, expressed in terms of the number of operations required to achieve a totally sorted record of length N. In this case, we applied a routine based on the C.A.R. Hoares's Quick Sort algorithm which is one of the most efficient sorting algorithms presenting an average complexity of the order $\mathcal{O}(N\log_2 N)$ and is adequate for our OS estimation purposes [59][60].

5.3.4   CDF based digital pre-distortion

The simplest way to apply digital pre-distortion can now be described using Order Statistics estimation of CDFs:

Step 1: The amplitude values from the sorted vector $\mathbf{x}'_{in[N]}$ are distributed along the vertical axis as presented in figure 5.8. The resulting is an estimate of $F_{in}^{-1}(x)$, whose input variable x is the normalized index (n/N) and its output is the corresponding amplitude value $x'_{in(n)}$. Thus we obtain an estimated $\widehat{F}_{in}^{-1}(\cdot)$ for the composition expressed in (5.29). Such estimation correspond to the set of coordinates

$$\widehat{\boldsymbol{F}}_{in[N]}^{-1} = \left[(1/N, x'_{in(1)}) \cdots (N/N, x'_{in(N)}) \right]. \tag{5.39}$$

Step 2: The sorted vector of distorted samples $\boldsymbol{x}'_{out[N]}$ returns N percentile values which are distributed this time throughout the horizontal axis (as opposed to figure 5.8). The resulting function is the estimated $\widehat{F}_{out}(x)$ constructed from the coordinate set

$$\widehat{\boldsymbol{F}}_{out[N]} = \left[(x'_{out(1)}, 1/N) \cdots (x'_{out(N)}, N/N) \right]. \tag{5.40}$$

Step 3: The final estimated pre-distortion curve is obtained through the composition of the two previous estimates. Thus, pre-distortion is equivalent to the linear interpolation of the input data with these sorted vectors. The composition $\widehat{\boldsymbol{F}}^{-1}_{in[N]}\left(\widehat{\boldsymbol{F}}_{out[N]}(\cdot)\right)$ gives a new set of coordinates defining an inverse for the non-linear transfer function $x_{out} = A[x_{in}]$ as follows:

$$\widehat{\mathbf{A}}^{-1}_{[N']} = \left[(x'_{out(1)}, x'_{in(1)}) \cdots (x'_{out(N')}, x'_{in(N')}) \right]^T \tag{5.41}$$

where $N' \leq N$ refers to an eventual decreased length due to the reduction of repeated coordinates $(x'_{out(n)}, x'_{in(n)}) = (x'_{out(n+1)}, x'_{in(n+1)})$, since they constitute nuisance information for the composition of an interpolation curve.

Regarding the composition of $A^{-1}[\cdot]$ expressed in (5.29), we can observe that the main advantage of an OS based AM/AM pre-distortion is that it does not require the time delay estimation when it is defined through the separate estimation of the input and output CDFs. However, in the relatively simplistic formulation above, the assumption of a perfect time alignment is desirable to achieve a good estimation of the PD characteristic. This means that the construction in (5.41) is the simple input-induced sampling of the HPA in base-band and hence, resorting to such statistical identification theory seems unreasonable since it involves a penalty in computational burden. This is, quoting a previously received (and very welcomed) criticism, analogous to "shooting a mosquito with a cannon ball". Nevertheless, this drawback disappears when we consider estimating the statistical distributions separately using independent data sets from the input and output of the HPA, and then perform the composition in (5.29). One alternative is to take the CDF estimations obtained by means of OS and perform a regression of the N' coordinates (which are excessive for interpolation) to a reduced set of, say, 32 or 64 coordinates to describe $\widehat{F}^{-1}_{in}(\cdot)$ and $\widehat{F}_{out}(\cdot)$. Another alternative to estimate these significant distributions is the use of the so-called Soft Histogram (SH) technique [61], which is based on information distribution methods and fuzzy bounded intervals for the histogram. However, when using alternatively the OS or SH methods, two comparative disadvantages arise. In SH the accuracy of the estimated curve is highly affected when some histogram intervals are poorly activated, therefore the number of bins and their width must be adaptive to the data density, which is computationally more complex compared to the self-adaptive property of the OS. Besides this, the SH implementation requires larger sample vectors than OS to achieve similar CDF estimation performance. Anyway, regardless of the chosen CDF estimation technique, the composition of the inverse AM/AM function results independent from the time delays between input and

output data. Additionally, as will be seen in the next chapter, the suitable use of OS can provide a rapid means to establish good initial conditions for the coefficients that approach the PD characteristics in a more complete and accurate adaptive PD algorithm. Given such benefits, in some cases, the "OS cannon ball" may become justified.

Considering the correspondences shown in equations (5.22) and (5.23), for the application of (5.41) in AM/AM PD, we can assume availability of N-sample long vectors $\boldsymbol{u}_x$ and $\boldsymbol{u}_y$ with the modulus of input and distorted sampled signals respectively. The samples in these vectors are related through the non-linear distortion defined in (5.1). Then, assuming $\Delta = 0$ for simplicity and replacing the general notation in (5.41), we have

$$\widehat{\boldsymbol{A}}_{[N']}^{-1} = \left[(u'_{y(1)}, u'_{x(1)}) \cdots (u'_{y(N')}, x'_{x(N')}) \right] \tag{5.42}$$

with $\widehat{A}^{-1}(u)$ the estimated inverse AM/AM function of the HPA. This PD is equivalent to linear interpolation of the data through the coordinate set in (5.42). Unlike the former, AM/PM PD is applied as an additive pre-correction term over the input phase $\alpha_x(n)$ such that,

$$\alpha_{xPD}(n) = \alpha_x(n) - \widehat{\Phi}_{PD}[u_x(n)] \tag{5.43}$$

where, from (5.32) and assuming a perfectly compensated or null delay Δ, we have

$$\widehat{\Phi}_{PD}[u_x(n)] = \Phi[u_x(n)] = \alpha_y(n) - \alpha_x(n). \tag{5.44}$$

Here, $\widehat{\Phi}_{PD}[u_x(n)]$ is obtained by interpolation of the elements in $\boldsymbol{u}_x$ with respect to the set of coordinate points of the AM/PM curve given by

$$\widehat{\boldsymbol{\Phi}}_{[N']} = \left[(u'_{x(1)}, \Phi'_{(1)}) \cdots (u'_{x(N')}, \Phi'_{(N')}) \right] \tag{5.45}$$

where $u'_{x(n)}$ and $\Phi'_{(n)}$ are the sorted elements from the corresponding input amplitude and modulus-dependent phase distortion vectors. In these expressions we have assumed perfect synchronization between the signals, however, this is a critical impairment to the system. Some synchronization solutions to counteract this problem have been proposed in [54][39][38].

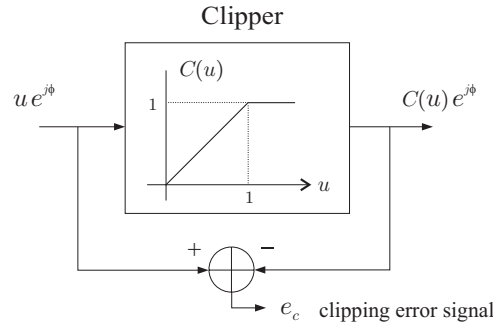# 5.A Appendix: Definition of a minimum error bound for a linear clipper with a Rayleigh distributed input

Figure 5.11: Measure of the I/O error signal for an ideal clipper.

Let us consider the ideal linear AM/AM clipper with unitary gain defined in (5.7). The ideal linear limiting device so defined only introduce input-to-output errors when the envelope of the input signal exceeds A_{sat}. Thence, with the resulting I/O error signal

$$e_c = (u - C(u))e^{j\phi}$$

measured as shown in figure 5.11, we can calculate the mean power of the clipping error signal as

$$\overline{P}_{Emin} = \int\limits_{A_{sat}}^{\infty} (u - A_{sat})^2 p(u) du \tag{5.46}$$

since, during saturation, $C(u) = A_{sat}$. In this integral expression, $p(u)$ is the probability density function of u. For this evaluation we are interested in a signal whose envelope follows a Rayleigh distribution whose corresponding PDF and CDF expressions where given in (5.2) and (5.3). Let us recall them here for convenience:

$$p_{Rayl}(u) = \frac{u}{\sigma^2}e^{-\frac{u^2}{2\sigma^2}}$$

$$F_{Rayl}(u) = 1 - e^{-\frac{u^2}{2\sigma^2}}.$$

Then, developing the square in (5.46) we have

$$
\begin{aligned}
\overline{P}_{Emin} &= \int\limits_{A_{sat}}^{\infty} (u - A_{sat})^2 p(u) du \\
&= \int\limits_{A_{sat}}^{\infty} \frac{u^3}{\sigma^2} e^{-\frac{u^2}{2\sigma^2}} du - 2A_{sat} \int\limits_{A_{sat}}^{\infty} \frac{u^2}{\sigma^2} e^{-\frac{u^2}{2\sigma^2}} du + A_{sat}^2 \int\limits_{A_{sat}}^{\infty} \frac{u}{\sigma^2} e^{-\frac{u^2}{2\sigma^2}} du.
\end{aligned}
\tag{5.47}
$$

The solution for the first integral term in (5.47) is

$$\int\limits_{A_{sat}}^{\infty} \frac{u^3}{\sigma^2} e^{-\frac{u^2}{2\sigma^2}} du = \left[-(u^2 + 2\sigma^2)e^{-\frac{u^2}{2\sigma^2}} \right]_{A_{sat}}^{\infty} = (A_{sat}^2 + 2\sigma^2)e^{-\frac{A_{sat}^2}{2\sigma^2}} \tag{5.48}$$

while the last term simply requires the direct evaluation of the Rayleigh CDF

$$A_{sat}^2 \int\limits_{A_{sat}}^{\infty} \frac{u}{\sigma^2} e^{-\frac{u^2}{2\sigma^2}} du = A_{sat}^2 \left[1 - e^{-\frac{u^2}{2\sigma^2}} \right]_{A_{sat}}^{\infty} = A_{sat}^2 e^{-\frac{A_{sat}^2}{2\sigma^2}}. \tag{5.49}$$

The second term can be solved by applying integration by parts where, for $\int x\,dy = xy - \int y\,dx$, the definitions

$$x = u \; ; \; dy = ue^{-\frac{u^2}{2\sigma^2}} \Leftrightarrow y = -\sigma^2 e^{-\frac{u^2}{2\sigma^2}}$$

yield the equivalence

$$
\begin{aligned}
2A_{sat} \int\limits_{A_{sat}}^{\infty} \frac{u^2}{\sigma^2} e^{-\frac{u^2}{2\sigma^2}} du &= \frac{2A_{sat}}{\sigma^2}\left(\left[-\sigma^2 u e^{-\frac{u^2}{2\sigma^2}} \right]_{A_{sat}}^{\infty} + \sigma^2 \int\limits_{A_{sat}}^{\infty} e^{-\frac{u^2}{2\sigma^2}} du \right) \\
&= 2A_{sat}\left(A_{sat} e^{-\frac{A_{sat}^2}{2\sigma^2}} + \sigma\sqrt{2} \int\limits_{\frac{A_{sat}}{\sigma\sqrt{2}}}^{\infty} e^{-\nu^2} d\nu \right) \\
&= 2A_{sat}^2 e^{-\frac{A_{sat}^2}{2\sigma^2}} + \sigma\sqrt{2\pi}A_{sat}\,\mathrm{erfc}\left(\frac{A_{sat}}{\sigma\sqrt{2}} \right).
\end{aligned}
\tag{5.50}
$$

Here, the change of variable $\nu = \frac{u}{\sigma\sqrt{2}}$ is done in order to include the complementary error function which is defined by

$$\mathrm{erfc}(x) = \frac{2}{\sqrt{\pi}} \int_x^{\infty} e^{-\nu^2} d\nu.$$

Thence, through the summation of (5.48), (5.49) and (5.50) according to (5.47) we obtain the total power of the clipping error signal as

$$\overline{P}_{Emin} = 2\sigma^2 e^{-\frac{A_{sat}^2}{2\sigma^2}} + \sigma\sqrt{2\pi}A_{sat}\,\mathrm{erfc}\left(\frac{A_{sat}}{\sigma\sqrt{2}} \right).$$

Finally, with this result, the minimum error bound for linearization, considering only clipping degradation for a Rayleygh distributed input signal with mean power $2\sigma^2$, can be obtained by calculating the ratio

$$(\overline{P}_{Emin}/\overline{P}_{in})[dB] = 10\log\left(\frac{\overline{P}_{Emin}}{\overline{P}_{in}} \right).$$